Nigerian Research Journal of Engineering and Environmental Sciences 8(2) 2023 pp. 517-525
p ISSN: 2635-3342; e ISSN: 2635-3350

Nigerian Research Journal of Engineering and Environmental Sciences
Journal homepage: www.rjees.com

Original Research Article

The Effects of Rain Attenuations in Satellite Communication System on C, Ku and Ka Frequency Bands

***[1]Udo, E.U., [2]Okpeki, U.K. and [3]Essien, U.J.**

[1]Department of Electrical/Electronic Engineering, Michael Okpara University of Agriculture, Umudike, Nigeria.
[2]Department of Electrical/Electronic Engineering, Delta State University, Oleh Campus, Abraka, Nigeria.
[3]Department of Electrical/Electronic Engineering, Akwa Ibom State Polytechnic, Ikot Osurua, Nigeria.
*thought.umoren@gmail.com

http://doi.org/10.5281/zenodo.10442763

ARTICLE INFORMATION

Article history:
Received 19 Sep. 2023
Revised 03 Nov. 2023
Accepted 10 Nov. 2023
Available online 30 Dec. 2023

Keywords:
Microwave frequency
Rain attenuation
Satellite communication
Atmospheric attenuation
Cloud

ABSTRACT

This paper presents the effects of rain attenuations on microwave frequency bands of C, Ku and Ka. The atmospheric attenuations such as rain, cloud, oxygen and water vapour have significant effect on the transmitting and receiving signals over satellite communication link, especially in locations prone to rainfall. This paper analyzed the effects of rain attenuation on satellite systems in selected areas in the city of Eket, Akwa Ibom State, Nigeria. The rain fall, cloud and gas data were measured and collected from the Nigerian meteorological agency for a period of six months to determine the frequency bands within the affected locations. MATLAB/Simulink and International telecommunication union radio communication (ITU-R) prediction model was employed to improve the received signals. The results obtained shows that for the exceedance time of 0.05 seconds, the attenuation values recorded during the rainfall at elevation angles of 10^0, 20^0, 30^0 and 40^0 are 10.16, 13.20, 19.28, 9.73, 12.59, 18.24, 10.46, 13.62, 19.99, 9.48, 12.23, 17.63, 9.15, 11.80, and 16.86 while for the exceedance time of 0.60 seconds, the attenuation values recorded at the same elevation angles are 1.09, 1.50, 2.38, 1.03, 1.42, 2.23, 1.12, 1.56, 2.49, 1.02, 1.37, 1.86, 0.96, 1.30 and 2.02. In conclusion, the effects of atmospheric attenuation that causes poor signal quality in the study area was minimized.

1. INTRODUCTION

The effect of rain attenuation is a primary issue when designing satellite-to-earth links operating at frequencies beyond 10 GHz. Droplets of rain absorb and scatter radio waves, leading to signal fading and decrease in the system reliability and availability. It also causes one of the major fundamental problems on the communication satellite links performance, resulting to large variations in the signal power at the receiver end. However, satellite services using 10 GHz frequencies and beyond are influenced by different propagation impairments like attenuation caused by rain, cloud and ice depolarization (Ezeh et al., 2014).

There are some basic effects of propagation abnormalities which affect the communication satellite systems performance. In a satellite communication, weather losses result from degradation of the satellite signals by hydrometers as they cross the earth's atmosphere. Some of the losses encountered by satellite communication systems are rain, cloud and gas attenuations. When higher frequencies are transmitted and received under heavy attenuations, signal degradation which is proportional to the intensity of propagation abnormalities occurs (Osahenvemwen and Omorogiuwa, 2017).

Satellite communications are essentially used for providing communication links between different areas on the earth by receiving information from a transmitting earth station. About 3,000 satellites are orbiting the earth relaying continuous and discrete information bearing data, video and audio from one location to another in the world (Harb et al., 2012).

Satellite based communication networks at high frequencies are rapidly expanding. These high frequency operations have enabled a large number of available applications and services including communications, navigation, telemedicine, remote sensing, network sensors distribution and access to internet without the use of wires (Udo and Odo, 2019). However, high frequency applications can generally result to large transmission problems because of atmospheric attenuations (Ezeh et al., 2014).

Most satellite functions effectively if the transmissions are directed to a desired area. When the desired area of coverage is focused, the emissions do not move away from the designated area and it minimizes the interference to the other systems. Without a functioning communication link, most satellites are rendered useless. To ensure a proper satellite to ground link, one has to make estimations of the signal attenuation because of the distance to the satellite, atmospheric distortions and other system specific losses. An important aspect is noise originating in the system components and from general background radiation (ITU-R, 2017).

The radio frequency in Ka band offers three advantages for satellite communication over the low frequencies of C and Ku bands in terms of spectrum availability, reduced interference potential and reduced equipment size. Satellite signals inevitably confront propagation impairments during signal transmissions between the satellite and earth stations. The Ka band is more susceptible to tropospheric impairments than lower frequencies which can degrade service quality. Rain, ice, fog, gas, clouds and moist air affect communication links in different ways. If estimation of such impairments can be done, proper mitigation techniques can be implemented to improve the quality of service (Sujimol et al., 2015).

Attenuation caused by rain, cloud and gas are primary sources of impairment to information propagation at millimeter and microwave wavebands. These impairments become particularly severe at higher frequencies, especially beyond Ku-band. Therefore, it is very difficult to maximally utilize satellite based network resources which are affected by weather attenuations (Al-Saegh et al., 2014).

Ishag et al., (2015) carried out a design and implementation of attenuation due to rain control and reduce simulation modules in MATLAB simulator. The method used investigated the Ku band signal efficiency under the rain attenuation effect. The results showed that the horizontally polarized signal was more attenuated by the rain than the circularly and vertically polarized signal.

Durodola et al., (2017) investigated rain effects on the performance of Ku-band satellite signals in Akure, Nigeria. Comparison of the predicted rain induced attenuation was estimated by applying the measured data was conducted with some chosen rain attenuation models like ITU-R, Garcia and Moupfouma. The results show the time series of rainfall during a typical rainy event is the reception pattern at Ku-band that indicated a very strong relationship between the reduction of the satellite signals and the rate of rainfall recorded.

The statement of the problem is that rain attenuations have a negative effect on the transmitting and receiving signals that leads to signal degradation due to heavy rainfall. The objective of the study is to use data from the Nigerian meteorological agency and determine the frequency bands that are suitable for satellite communications in the affected areas.

2. MATERIALS AND METHODS

2.1. Data Collection

The materials used in this paper include computer system, parabolic reflector antenna**,** coaxial cable**,** rain gauge**,** stopwatch**,** compass**,** radiosonde and MATLAB/Simulink**.** Data obtained from the Nigerian meteorological agency were analyzed for a period of six months starting from the month of April 2022 to October 2022. The rain attenuation model was implemented based on the modified ITU-R prediction model and its consists with different range with different elevation angles for various rain climates. The model is used for estimating long term statistics of rain attenuation at high frequencies of the affected regions. The model includes the fuzzy logic inference system which acts as a decision scheme to select and adjust the satellite connection to most bands that favors certain weather impairment within the selected location. The general satellite system model contains three main components such as the earth stations, satellites and the links between the channels and these was created using MATLAB/Simulink.

The city of Eket in Akwa Ibom State of Nigeria was chosen as a study area to investigate satellite attenuation and atmospheric condition that affects satellite communication with different bands in the area. Atmospheric condition of these areas such as rainfall rate, rain height above sea level, and liquid water content of rain drops, temperature and relative humidity were taken into consideration. The effect of raindrops was determined at higher transmission frequencies above 10 – 250 GHz. Figure 1 shows the flowchart of rain attenuation with fuzzy logic system.

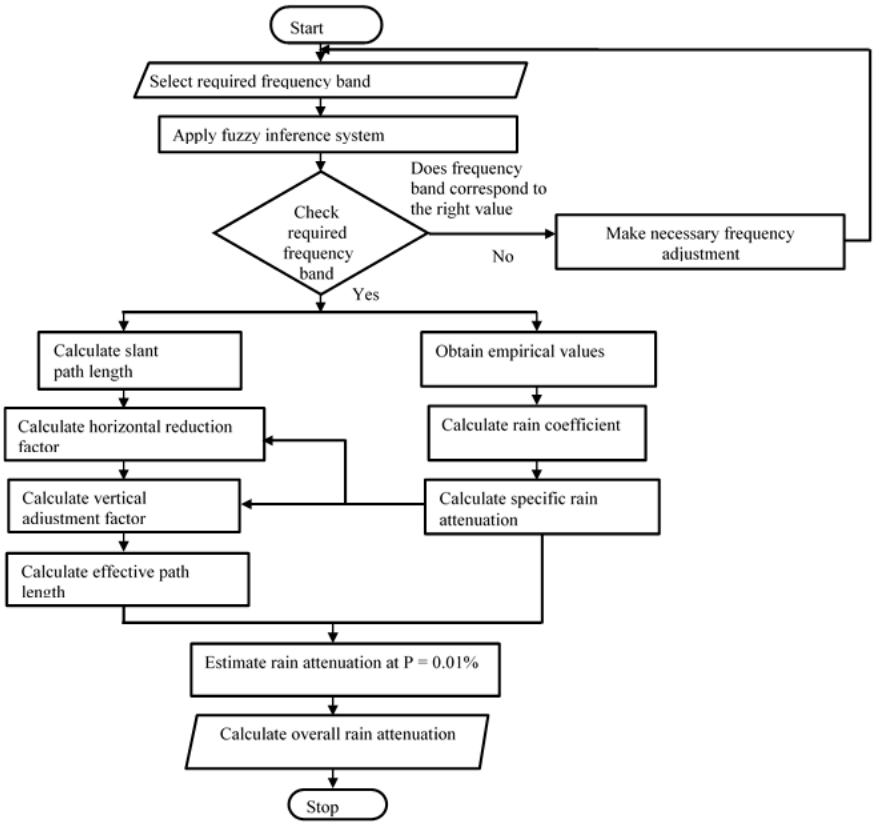

Figure 1: Flowchart of rain attenuation with fuzzy logic system

2.2. Modeling of the Rain Attenuation

The developed model performs two procedures simultaneously. The first technique starts by obtaining the frequency-dependent rain empirical values before calculating the rain-specific coefficients s and λ as shown in Equations (1) and (2).

$$s = \frac{s_H + s_V + (s_H - s_V)Cos^2\theta Cos2\tau}{2} \quad (1)$$

$$\lambda = \frac{s_H\lambda_h + s_v\lambda_v + (s_H\lambda_H - s_v\lambda_v)cos^2\theta\cos(2\tau)}{2k} \quad (2)$$

where τ is the polarization angle, θ is the elevation angle, ρ is the percentage of exceeding time and f is the operating frequency.

The specific rain attenuation per 1 km is calculated depending on the actual measured precipitation rate at p = 0.01% as shown in Equation (3).

$$\epsilon_{Rain} = \lambda(R_{0.01})^k \quad (3)$$

This value will be applied in the second method to identify the effective path length and to predict the overall rain attenuation. The horizontal reduction factor (s_H) for 0.01% at the time can be calculated using Equation (4).

$$s_H = \frac{1}{1+0.8\sqrt{\frac{P_H\epsilon_R}{f}} - 0.4\left(1-e^{-2P_H}\right)} \quad (4)$$

where P_H is the horizontal projection which depends on the slant path length T_L and the elevation angle θ as shown in Equation (5).

$$P_H = T_L\cos\theta \quad (5)$$

The slant path length depends on the vertical height from the earth station to the rain height as well as θ as shown in Equation (6).

$$T_L = \begin{cases} \frac{H_R - H_E}{\sin\theta} \\ \frac{2(H_R - H_E)}{\sqrt{sin^2\theta + \frac{2(H_R - H_E)}{B_R}} + \sin\theta} \end{cases} \quad (6)$$

Where H_R and H_E are the rain and earth station heights above sea level and B_R is the earth radius. The vertical adjustment factor C_F is calculated at 0.01% of the time using Equation (7).

$$C_F = \frac{1}{1+\sqrt{\sin\theta}\left[31\left(1-e^{\frac{\theta}{1-x}}\right)\frac{\sqrt{R_L\epsilon_R}}{f^2} - 0.45\right]} \quad (7)$$

The effective path length can be obtained using Equation (8) and the overall rain attenuation at p = 0.01% of time ($D_{0.01}$) is calculated in Equation (9).

$$P_L = R_L C_F \quad (8)$$

$$D_{0.01} = P_L\epsilon_R \quad (9)$$

2.3. Modeling of the Cloud Attenuation

The amount of liquid water content contained in the cloud is responsible for absorption and scattering of electromagnetic energy especially for frequencies above 10 GHz with less intensity than that of rain (Singh et al., 2017). Cloud attenuation such as signal frequency and elevation angle rests on the cloud parameters like average height, thickness, total content of liquid water and temperature. The cloud specific attenuation coefficient is calculated using Equation (10).

$$\epsilon_{cloud} = \frac{0.820f}{e^{"}\left[1-\left(\frac{2+e'}{e"}\right)^2\right]} \tag{10}$$

Where ϵ_{cloud} is the cloud specific attenuation coefficient and f is the frequency

2.4. Oxygen and Water Vapour Attenuations

The effective water vapour path length is based on the exponential atmosphere that describe the relation between water vapour density and altitude. The water vapour specific attenuation in (dB/km) is calculated as shown in Equation (11).

$$\epsilon_w = f^2 s_T^{2.5} \rho [v_1 + v_3 + v_4 + v_5 + v_6 + v_7 + v_8 + v_9] \times 10^{-4} \tag{11}$$

Where ϵ_w is the water vapour specific attenuation, f is the frequency, s_T is the altitude reduction factor, ρ is the percentage of exceedance time and v is the water vapour density.

The total gas attenuation for oxygen and water vapour attenuations can be predicted using Equation (12).

$$\mathrm{T_A} = \frac{\mathrm{T_o + T_w}}{\sin\theta} \tag{12}$$

where $\mathrm{T_A}$ is the total gas attenuation, To is the total amount of oxygen and $\mathrm{T_W}$ is the total water vapour attenuation.

3. RESULTS AND DISCUSSION

The percentage of exceedance time for rain attenuation was tabulated from 0.01 to 1.00 seconds for various elevation angles of 10, 20, 30, 40 and 50 degrees at C, Ku and Ka bands. Table 1 presents the rain attenuation values at various frequency bands for different elevation angle. The results revealed that, the higher the elevation angle, the lower the attenuation and therefore the higher the values of Eb/No. Again, it was also observed that, bad weather attenuates satellite transmission to a large extent at the study area. This is because during heavy rainfall, bad channel quality imposes serious problems to the users of the satellite network. This leads to communication link outage at lower elevation angles θ. The elevation angle depends on the Eb/No along with the transmission bit rate and bandwidth.

Figures 2 to 6 showed that the higher the percentage of exceedance time, the lower the attenuation. Similarly, for the given elevation angle of rainy weather events, the higher the attenuation, the lower the elevation angle, the higher the rain Eb/No. The plot of Eb/No with rainfall at 10° elevation angle is shown in Figure 2. It is observed from the plot that at 0.1, the values of Eb/No are 4 dB, 5 dB and 7.5 dB. Again, at 0.5, the values of Eb/No are 1 dB, 2 dB, 3 dB. Also, at 1 dB, the values of Eb/No are 1 dB, 1 dB, 2 dB. This shows that an increase in the percentage of exceedance time lowers the attenuation. The plot of Eb/No with rainfall events at 20° elevation angle is shown in Figure 3. It is observed from the plot that at 0.1, the values of Eb/No are 3.5 dB, 4.5 dB and 7 dB. Also, at 0.5 the values of Eb/No are 1.5 dB, 2 dB and 3 dB. Again, at 1 dB, the values of Eb/No are 1 dB, 1 dB, 2 dB.This indicates that an increase in the percentage of exceedance time lowers the attenuation. The plot of Eb/No with rainfall events at 30° elevation angle is shown in Figure 4. It is observed from the plot that at 0.1, the values of Eb/No are 4 dB, 5 dB and 8 dB. Also, at 0.5, the values of Eb/No are 1.5 dB, 2 dB and 3 dB. Again, at 1 dB, the values of Eb/No are 1 dB, 1 dB, 2 dB. This shows that an increase in the percentage of exceedance time lowers the attenuation.

Table 1: Rain attenuation values at C, Ku and Ka bands at different elevation angles

Percentage of exceedance time	@ Elevation angle =10 degree			@ Elevation angle =20 degree			@ Elevation angle =30 degree			@ Elevation angle =40 degree			@ Elevation angle =50 degree		
	C	Ku	Ka	C	Ku	Ka	C	Ku	Ka	C	Ku	Ka	C	Ku	Ka
0.01	14.04	17.84	25.32	13.45	17.67	24.05	14.37	18.36	26.19	13.12	16.62	23.31	12.70	16.04	22.36
0.02	12.45	16.05	22.99	11.94	15.29	21.80	12.81	16.49	23.81	11.65	14.87	21.11	11.26	14.34	20.22
0.03	11.46	14.81	21.42	10.99	14.13	20.29	11.79	15.25	22.18	10.71	13.73	19.63	10.34	13.23	18.79
0.04	10.74	13.91	20.23	10.28	13.27	19.15	11.04	14.34	20.97	10.02	12.89	18.52	9.67	12.41	17.71
0.05	10.16	13.20	19.28	9.73	12.59	18.24	10.46	13.62	19.99	9.48	12.23	17.63	9.15	11.80	16.86
0.06	9.70	12.62	18.49	9.28	12.03	17.49	9.98	13.02	19.18	9.03	11.69	16.90	8.72	11.24	16.15
0.07	9.30	12.13	17.88	8.90	11.56	16.84	9.57	12.52	18.49	8.66	11.23	16.28	8.36	10.80	15.55
0.08	8.96	11.71	17.24	8.58	11.15	16.29	9.22	12.08	17.89	8.34	10.83	15.73	8.05	10.41	15.03
0.09	8.66	11.33	16.72	8.28	10.79	15.79	8.92	11.70	17.35	8.06	10.48	15.25	7.77	9.77	14.57
0.01	8.40	11.00	16.26	8.03	10.47	15.35	8.66	11.36	16.88	7.81	10.16	14.83	7.53	7.85	14.16
0.02	6.71	8.87	13.27	6.41	8.42	12.50	6.92	9.16	13.79	6.23	8.17	12.06	6.00	6.79	11.50
0.03	5.79	7.69	11.59	5.53	7.31	10.92	5.98	7.96	12.06	5.37	7.08	10.52	5.17	6.09	10.03
0.04	5.18	6.90	10.46	4.94	6.55	9.84	5.35	7.14	10.88	4.80	6.35	9.48	4.62	5.56	9.03
0.05	4.73	6.32	9.61	4.51	5.99	9.03	4.88	6.54	10.05	4.38	5.81	8.70	4.21	5.15	8.28
0.06	4.38	5.86	8.94	4.17	5.56	8.40	4.52	6.06	9.31	4.05	5.38	8.09	3.89	4.82	7.69
0.07	4.09	5.48	8.39	3.89	5.19	7.88	4.22	5.68	8.74	3.78	5.03	7.59	3.63	4.54	7.21
0.08	3.85	5.17	7.93	3.66	4.90	7.44	3.97	5.35	8.25	3.55	4.74	7.16	3.41	4.30	6.81
0.09	3.64	4.90	7.52	3.46	4.64	7.06	3.76	5.07	7.84	3.36	4.49	6.80	3.23	4.09	6.46
0.10	3.46	4.66	7.18	3.29	4.41	6.74	3.57	4.83	7.48	3.19	4.27	6.48	3.07	3.83	6.16
0.20	2.39	3.25	5.07	2.28	3.07	4.75	2.48	3.37	5.29	2.21	2.97	4.57	2.12	2.84	4.33
0.30	1.86	2.54	3.99	1.77	2.40	3.73	1.93	2.64	4.16	1.71	2.32	3.58	1.64	2.22	3.40
0.40	1.52	2.08	3.28	1.44	1.97	3.07	1.57	2.16	3.43	1.40	1.90	2.95	1.34	1.81	2.79
0.50	1.28	1.75	2.77	1.21	1.65	2.59	1.32	1.82	2.90	1.17	1.60	2.49	1.12	1.52	2.36
0.60	1.09	1.51	2.38	1.03	1.42	2.23	1.12	1.56	2.49	1.02	1.37	1.86	0.96	1.30	2.02
0.70	0.95	1.31	2.07	0.89	1.23	1.93	0.98	1.35	2.17	0.86	1.18	1.86	0.83	1.13	1.76
0.80	0.82	1.13	1.82	0.78	1.07	1.69	0.85	1.04	1.90	0.75	1.03	1.63	0.72	0.99	1.54
0.90	0.72	1.09	1.60	0.69	0.94	1.49	0.75	0.92	1.67	0.66	0.91	1.43	0.63	0.87	1.36
1.00	0.64	0.89	1.42	0.61	0.83	1.32	0.62	0.91	1.48	0.59	0.80	1.27	0.56	0.77	1.21

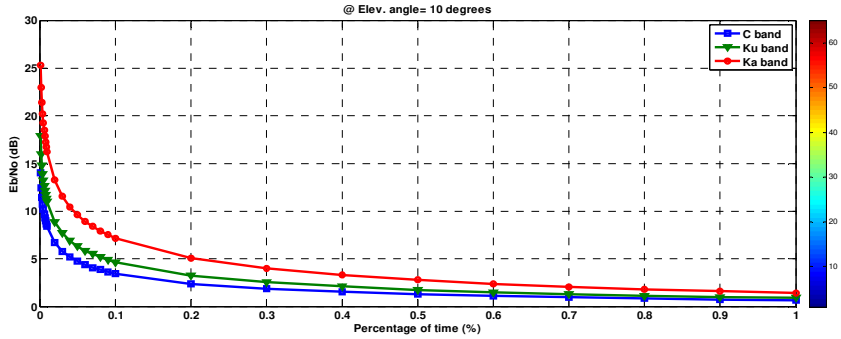

Figure 2: Plot of Eb/No against percentage of time at 10º elevation angle

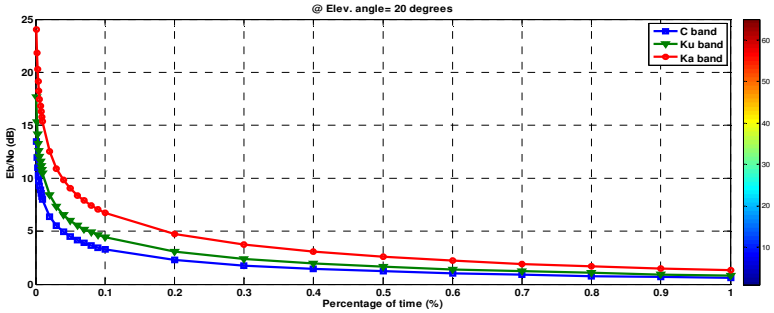

Figure 3: Plot of Eb/No against percentage of time at 20º elevation angle

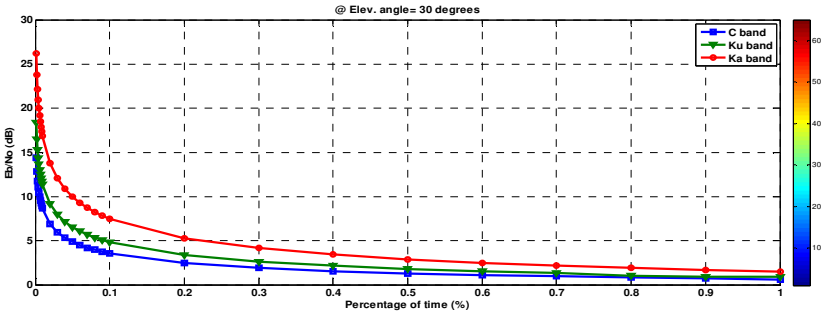

Figure 4: Plot of Eb/No against percentage of time at 30º elevation angle

The plot of Eb/No with rainfall events at 40º elevation angle is shown in Figure 5. It is seen from the plot that at 0.1, the values of Eb/No are 3.5 dB, 4.5 dB and 6 dB. Again, at 0.5, the values of Eb/No are 1.5 dB, 2 dB and 3 dB. Also, at 1 dB, the values of Eb/No are 1 dB, 1 dB, 2 dB. This indicates that an increase in the percentage of exceedance time lowers the attenuation. The plot of Eb/No with rainfall events at 50º elevation angle is shown in Figure 6. It is observed from the plot that at 0.1, the values of Eb/No are 3 dB, 4 dB and 6 dB. Again, at 0.5 the values of Eb/No are 1.5 dB, 2 dB and 3 dB. Also, at 1 dB the values of Eb/No are 1 dB, 1 dB, 2 dB. This shows that an increase in the percentage of exceedance time lowers the attenuation. The significant amount of dry air and water vapour attenuation appears at specific regions across the frequency spectrum of the affected locations in Eket. The total correlated gases attenuation at various relative humidity is shown in Figure 7. The gas attenuation increases as frequency increases from 250 GHz for a significant increase in relative humidity of the gases. The specific gas attenuation started at frequencies above 100 GHz due to the effect of oxygen before the attenuation level went down. The effect also took part at frequencies above 210, 310 and 410 GHz through the fuzzy logic inference system. This effect occurs due to water vapour attenuation using fuzzy logic system with varying relative humidity.

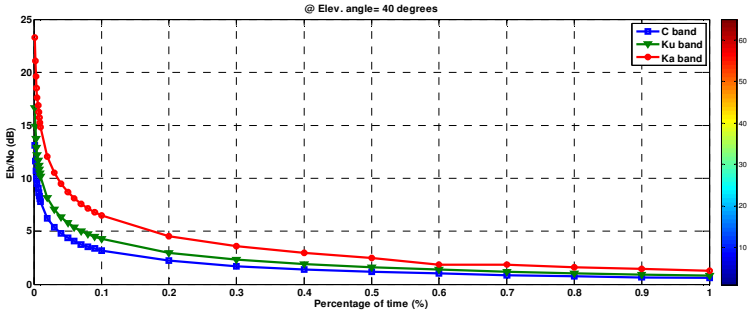

Figure 5: Plot of Eb/No against the percentage of time at 40º elevation angle

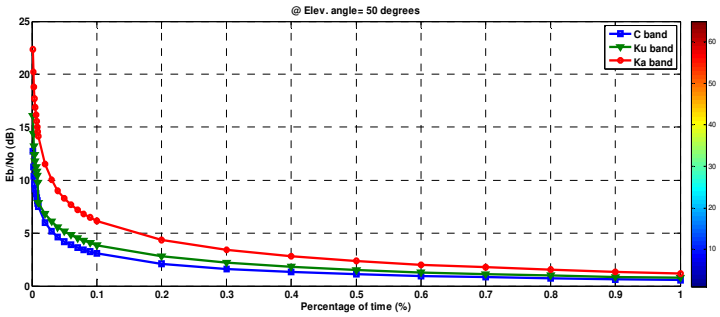

Figure 6: Plot of Eb/No against percentage of time at 50º elevation angle

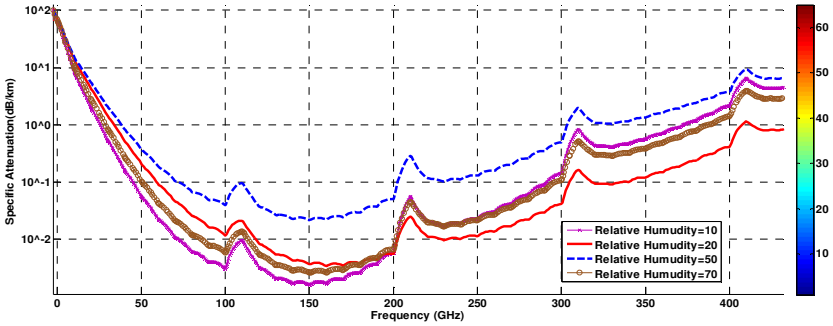

Figure 7: Gas attenuation at various relative humidity

4. CONCLUSION

The effect of rain attenuation due to poor signal quality was improved through the simulated and prediction models for rain, cloud and gas attenuation. The gas attenuation at fixed 50% relative humility has reached higher level of 415 GHz. The relative humidity is directly proportional to the amount of signal power attenuation due to the water vapour particles in space and the total gas attenuation. However, the locations of Ikot Akpan Ishiet and Awa Iman in the study area usually suffer from higher relative humility which indicates increased in gas attenuation. However, proper implementation of the attenuation model in the affected locations helps to initiate the selection of the frequency band that best suite transmission. The plots of attenuation against the percentage of exceedance time decreases at various rainfall events on C, Ku and Ka frequency bands at 10 ºC, 20 ºC, 30 ºC, 40 ºC and 50 ºC and these indicates that an increase in the percentage of exceedance lowers the attenuation signal.

5. ACKNOWLEDGMENT

I wish to acknowledge the staff of the Nigerian meteorological agency in Akwa Ibom State for their support in providing the needed data for the success of this paper.

6. CONFLICT OF INTEREST

There is no conflict of interest associated with this work.

REFERENCES

Al-Saegh, A. M., Sali, A., Ismail, A. and Mandeep, J. S. (2014). Analysis and Modeling of the Cloud Impairments of Satellite-to-land Mobile Channel at Ku and Ka Bands. *7th Advanced Satellite Multimedia Systems Conference and the 13th Signal Processing for Space Communications Workshop*, pp. 436–441.

Durodola, O. M., Ojo, J. S. and Ajewole, M. O. (2017). Performance of Ku-band Satellite Signals Received During Rainy Condition in two Low Latitude Tropical Locations of Nigeria. *Adamawa state university journal of scientific research*, 1(5), pp. 1-17.

Ezeh, G. N., Chukwuneke, N. S, Ogujiofor, N. C, Diala, H. (2014). Effects of Rain Attenuation on Satellite Communication Link. *Advances in Sciences and Technology Research Journal*, 8(22), pp. 1-11.

Harb, K., Yu, F. R. and Abdul-Jauwad, S. (2012). Performance Evolution in Satellite Communication Networks along Markovian Channel Prediction. *Journal of wireless networking and communications,* 2(5), pp. 143-157.

Ishag, I. O., Abdalla, A. G. and Mustafa, A. B. (2015). Reduce and Control the Impact of Rain Attenuation for Ku Band in Sudan. *International journal of engineering, applied and management sciences paradigms*, 21(01), pp. 1-6.

ITU-R, (2017). Propagation Data and Prediction Methods required for the Design of Earth-space Telecommunication Systems. ITU Radio communication assembly, pp. 1-28.

Osahenvemwen, O. A. and Omorogiuwa, O. (2017). Rain Attenuation Analysis from System at Ka and Ku frequency Bands. *American journal of advanced research*, 1, pp. 7-12.

Singh, H., Kumar, R., Bonev, B. and Petkov, P. (2017). Cloud Attenuation Issues in Satellite Communications at Millimeter Frequency Bands-state of Art. *International journal of scientific and operating engineering research*, 8(7), pp. 858–862.

Sujimol, M. R., Acharya, R., Singh, G. and Gupta, R. K. (2015). Rain Attenuation using Ka and Ku Band Frequency Beacons at Delhi Earth Station. *Indian journal of radio and space physics*, 44, pp. 45-50.

Udo, E. U. and Odo, K.O. (2019). Performance Improvement of Signal over Ku-band Satellite Communication using Fuzzy logic system. Proceedings of Engineering for Sustainable Economic Diversification, Food and National Security, pp. 301-314.